Software tools for thermodynamic calculation of mechanically unstable phases from first-principles data

Sara Kadkhodaei and Axel van de Walle

School of Engineering, Brown University, Providence, RI 02912

Abstract

This paper introduces the P^4 software package, a set of software tools that automate the process of vibrational free energy calculation for mechanically unstable phases. The Piecewise Polynomial Potential Partitioning (P^4) method is a recently developed method that tackles the issue of phonon instabilities in solid solutions and compounds. The method efficiently explores the system's *ab-initio* energy surface by discrete sampling of local minima, which is combined with a continuous sampling of the vicinity of these local minima via a constrained harmonic lattice dynamic approach. The free energy values obtained by this toolkit can be used in thermodynamic assessments and phase diagram calculations. As a unique advantage, it provides the tool to calculate the vibrational free energy in a wide composition range in alloys. This feature is not practically achievable by relying only on brute-force molecular dynamics or random sampling techniques.

Keywords: Statistical Physics and Thermodynamics, Anharmonic lattice dynamics, Software, Free energy calculation, Phonon instability, First-principles calculation

PROGRAM SUMMARY

Program Title: P^4 (Piecewise Polynomial Potential Partitioning)
Licensing provisions: CC by 4.0
Programming language: C++ and Bash
Program Files: http://go.uic.edu/p4 or doi: https://doi.org/10.26300/zs0n-2c84
Nature of problem: A number of technologically relevant materials become thermodynamically stable at high enough temperatures in spite of existing phonon instabilities. This makes the standard lattice dynamics approaches insufficient to describe stabilizing entropy effects in these materials.
Solution method: We implement the Piecewise Polynomial Potential Partitioning method [1] which facilitates thermodynamic calculations in mechanically unstable materials that are stabilized at finite temperatures due to anharmonic entropy effect. The current version of our model interfaces with density functional theory code VASP [2].
Additional comments including Restrictions and Unusual features: The P^4 code needs to be built into the ATAT toolkit [3]. The instruction on how to install P^4 into the ATAT toolkit is given in the documentation.

[1] Sara Kadkhodaei, Qi-Jun Hong, and Axel van de Walle, *Free energy calculation of mechanically unstable but dynamically stabilized bcc titanium.*Phys. Rev. B, 95 (2017) 064101
[2] G. Kresse and J. Furthmuller, *Efficient iterative schemes for ab initio total-energy calculations using a plane-wave basis set.* Phys. Rev. B 54 (1996) 11169
[3] A. van de Walle and M. Asta and G. Ceder, *The alloy theoretic automated toolkit: A user guide.* Calphad 26 (2002) 539–553

1. Introduction

First-principles quantum mechanical technique based on density functional theory has progressed significantly over the last few decades and has proven to be a viable tool to predict thermodynamic properties with an accuracy comparable to experimental uncertainties [1–3]. The integration of first-principles calculations into the CALPHAD framework is an established technique [4] that facilitates phase stability calculations for technologically important

engineering materials in different phases. However, the underlying "phase stability" assumption in CALPHAD approaches requires a single stable lattice to represent the material's crystal structure. This assumption reduces the applicability of the aforementioned frameworks, since the crystal structure of many high-temperature phases exhibit mechanical instabilities. These mechanical instabilities are common among a number of solid state systems, such as many transition metals [5, 6], shape-memory alloys [7–9], refractory oxides [10] and ferroelectric materials [11].

In this work, we present a set of software tools in the P^4 software package [12], based on our recently developed P^4 method [5, 7]. The P^4 method circumvents the "lattice stability" limitation by introducing an augmented lattice for a crystal structure with phonon instabilities. The P^4 software toolkit enables the incorporation of first-principles input within the CALPHAD framework for a phase with mechanical instabilities that is stabilized at finite temperature.

One major advantage of the P^4 method is the simultaneous incorporation of anharmonic vibrational and configurational entropic effects. This advantage arises from the combined use of coarse graining of partition function and cluster expansion technique [13, 14], which enables an efficient representation of *ab initio* free energy in terms of cluster interactions for a desired composition range in solid solutions. Therefore, the P^4 method facilitates the free energy calculation in solid solution with anharmonic vibrational effects along a wide composition range. It provides a more practical approach for alloy thermodynamic calculations compared to methods based on molecular dynamics or brute-force random sampling techniques [8, 15, 16].

Aside from the P^4 method, a number of methods have been devised to tackle the problem of mechanical instabilities due to anharmonic lattice dynamics. Self-consistent *ab initio* lattice dynamics (SCAILD) method offers a computationally inexpensive model for predicting effective finite-temperature phonon frequencies and free energies in a range of systems [17, 18]. Stochastic self-consistent harmonic approximation (SSCHA) method is a variational approach in which an anharmonic free energy is obtained by optimizing it with respect to all independent variables in a trial harmonic potential including phonons, polarization vectors (eigenvectors) and structural parameters of the crystal [19]. Alternatively, temperature dependent effective potential (TDEP) methods obtain the finite-temperature phonon frequencies by fitting *ab initio* molecular dynamics (AIMD) forces to the forces described in the harmonic approximation [20–22]. In other words, it determines the best harmonic fit to anharmonic energy surface. SCAILD, SSCHA, TDEP, and, more generally, self-consistent harmonic approximation (SCHA) approaches, fundamentally rely on the existence of an effective harmonic potential for the energy surface. If this assumption is inappropriate, there is no systematic way to improve the accuracy of the model. Moreover, TDEP methods rely on AIMD calculations that can become computationally intractable when anharmonic effects are sufficiently strong to trap the system in local minima for extended times. Effective Hamiltonian approaches offers a systematically improvable model by explicit parametrization of the system's anharmonic energy surface [23, 24]. Anharmonic vibrational effects in free energy can then be accounted for through thermodynamic integration on the anharmonic energy surface. However, the task of parametrizing the relevant anharmonic degrees of freedom in effective Hamiltonian approaches can become daunting as the range of interactions increases or as the number of components increases.

A number of software toolkits have been implemented based on the aforementioned approaches. The `scph` code has been implemented based on SCAILD method, where the effective phonon spectrum is solved for self-consistently [25]. Additionally, `TDEP` [26] and `ThermoPhonon` [27] have been implemented based on TDEP approach to calculate temperature dependent phonons by minimizing the difference between AIMD forces and an effective force constant. The P^4 toolkit can be distinguished from the aforementioned toolkits in two aspects. First, the P4 toolkit offers a model with systematically improvable accuracy above an effective harmonic model while it only requires *ab initio* calculation of harmonic forces. The system energy surface is approximated with a piecewise quadratic potential in which the accuracy can be improved by increasing the number of pieces. Second, in the P4 method the anharmonic vibration effects are incorporated into a cluster expansion framework, thus facilitating modeling the coupling between anharmonic lattice vibrations and the chemistry of the system..

In the following sections, we provide a brief description of the theoretical framework of the P^4 method [5, 7], a concise user guide to the P^4 software toolkit, a detailed description of the implementation of the P^4 toolkit, and finally a prototypical example to illustrate the usage of the P^4 toolkit. One can access the code and its manual at https://go.uic.edu/p4 or https://doi.org/10.26300/zs0n-2c84.

2. Theoretical framework

2.1. Piecewise polynomial potential partitioning

The existence of a thermodynamically stable crystal structure with phonon instabilities at high enough temperature implies that anharmonic entropy effects result in "dynamical stabilization" of the mechanically unstable phase. In this case, the system lacks a single representative stable crystal structure within the harmonic approximation. However, its structure can be described by anharmonic dynamic fluctuations among "local low-symmetry distortions" while maintaining a high-symmetry time-averaged structure. These anharmonic vibrations have entropic stabilizing effects beyond the harmonic vibration contributions. From this perspective, the high symmetry structure is only one of the possible configurational states among multiple low-symmetry configurational states accessible to the system. The P^4 method implements this notion by creating an augmented lattice, denoted by L_{aug}, that is associated with the mechanically unstable crystal lattice. The augmented lattice has the same unit cell as the unstable crystal lattice. However, it includes extra lattice points in addition to the high-symmetry lattice sites. These extra lattice points are located at nearby possible atomic positions that may become occupied as the system visits many possible low-symmetry distortions (see Fig. 2). Any possible arrangement of atomic species on the augmented lattice is called a configuration and is denoted by σ. The Helmholtz free energy associated with the mechanically unstable phase can be obtained by coarse-graining of the partition function [13] according to the following equation,

$$F_{L_{aug}} = -k_B T \ln \sum_{\sigma \in L_{aug}} \exp(-\beta F^*_\sigma), \tag{1}$$

where

$$F^*_\sigma = -k_B T \ln \int_{\boldsymbol{x} \in \zeta_\sigma} \exp(-\beta V(\boldsymbol{x})) d\boldsymbol{x}, \tag{2}$$

where $\beta = 1/(k_B T)$, T is temperature, k_B is Boltzmann's constant, $\boldsymbol{x}$ is a $3N$ vector of all atomic positions, N is the number of atoms in the system, ζ_σ is the neighborhood of configuration σ, which is defined formally below, and $V(\boldsymbol{x})$ is the potential energy of the system at a state represented by the position vector $\boldsymbol{x}$. In Eq. 2, $V(\boldsymbol{x})$ is approximated by a quadratic polynomial, which is expanded about $\boldsymbol{x}^r_\sigma$. $\boldsymbol{x}^r_\sigma$ is the location of the minimum within ζ_σ. The integral domain in Eq. 2 confines the integration to ζ_σ, as each quadratic polynomial potential $V(\boldsymbol{x})$ is specific to the domain ζ_σ. We use the cluster expansion formalism [14] in order to represent the constrained vibrational free energy, denote by F^*_σ, as a polynomial series in terms of the occupation variable of each augmented lattice site i, denoted by σ_i.

$$\frac{F^*_\sigma(T)}{N_s} = \sum_\alpha m_\alpha J_\alpha(T) \left\langle \prod_{i \in \alpha} \sigma_i \right\rangle_{\alpha'} \tag{3}$$

The above sum is over symmetrically distinct clusters α, while the average is over clusters α', which are symmetrically equivalent to α. N_s is the number of sites in the augmented lattice, m_α is the multiplicity of cluster α and $J_\alpha(T)$ is the effective cluster interaction (ECI) of cluster α at temperature T. The ECIs are the polynomial series coefficients and are determined via the fitting of the above series to the calculated F^*_σ at different temperatures.

2.2. Implementation details

We define ζ_σ as the Cartesian product of tridimensional Voronoi cells associated with each site in the augmented lattice. The Voronoi cells are generated by Voronoi tessellation in tridimensional space, using the augmented lattice sites as the generators (see Fig. 3(a)). This definition implicitly excludes those unphysical high energy vibrational states where two or more atoms would lie in the same tridimensional Voronoi cell of a given lattice site (see Ref. [5] for more details).

We refer to each augmentation of lattice sites (a high-symmetry lattice point and local lower-symmetry distortions) in the augmented lattice as a "group" of site. In order to mimic the fluctuation of the system among local distortions, in any configuration σ in Eq. 1, each "group" of sites is only occupied by one atomic species and the rest of the sites in the "group" are vacant. This notion is consistent with the way ζ_σ is defined in terms of avoiding configurations with more than one atom occupying each "group" of sites. To avoid performing *ab initio* calculations for these unphysical states, the ECIs for clusters that are formed by sites inside each "group" are set to pre-specified values in a way to suppress the appearance of these states (see the following sections for more details).

3. Usage

The process consists of five main steps: (i) build an augmented lattice that corresponds to the high-symmetry unstable crystal lattice, (ii) generate crystal structures with desired concentrations on the augmented lattice, (iii) obtain the confined relaxed atomic position of each structure and its corresponding energy and energy derivatives via *ab-inito* methods, (iv) obtain the vibrational free energy associated with each structure on the augmented lattice, and (v) calculate the vibrational free energy associated with the mechanically unstable crystal structure. The aforementioned steps are described in more details in the following sections by only considering the simplest use of the commands in the P^4 toolkit. More options are available, which are described in each command's help file. In the descriptions below, strings enclosed in brackets [] need to be replaced by suitable user input without the brackets. The P^4 package performs as an embedded tool into the widely used `ATAT` toolkit [28, 29] for convenience of the users. All the input and output files generated by this toolkit are transferable to the `ATAT` toolkit. In Fig. 1, a summary of the calculation steps in the P^4 package and the transfer of the output of P^4 into an input to `ATAT` are shown.

3.1. Augmented lattice generation

The following command generates an augmented lattice given the high symmetry unstable crystal lattice and a nearby local distortion structure.

```
auglat -l=[unstable lattice file name] -loc=[local distortion structure file name] -ol=[output augmented lattice file name]
```

The format for the lattice and structure files are described in details in the command help (see `auglat -h`) and in Appendix A. The underlying assumption in the P^4 method is that the high-symmetry crystal structure is described as a dynamic fluctuation of the system among local distortions. Given one possible nearby distortion, the code will generate the augmented lattice by considering all distortions that are symmetrically equivalent to the given distortion (for example, see table 1 and Fig. 2). If the provided local distortion structure is too distorted with respect to the high-symmetry crystal structure, the code will generate an error. A distortion is considered too large when the local structure atomic positions are not closest to the their corresponding high-symmetry atomic positions. For example, if the distorted atomic position of the first lattice site in the high-symmetry lattice is closer to any high-symmetry lattice point other than the first lattice point position, it is considered a too large distortion. The phonon instabilities of the high-symmetry crystal provide a guide to identify the corresponding local distortion (see Ref. [5, 7]). For example, the longitudinal acoustic phonon located at 2/3 [$\xi\xi\xi$] branch in bcc phase of Ti points to a local minimum along the trigonal distortion path, which is used to build the augmented lattice for the bcc crystal structure of Ti.

3.2. Structure generation on the augmented lattice

The following command generates an atomic structure on the augmented lattice.

```
genrndstr -lhs=[unstable lattice file name] -laug=[augmented lattice file name] -os=[output structure file name] -ss=[n1,n2,n3]
```

The `-ss` option determines the size of the supercell as three integer numbers n_1 to n_3, where n_1 specifies unit cell repetitions along the first coordinate, etc. The unit cell is defined in the lattice files. The code automatically prevents the occupation of a "group" of sites in the augmented lattice by more than one atomic species (see Fig. 2). The command generates structures randomly by considering the possible atomic types on each lattice sites determined in the lattice files (see `auglat -h` or Appendix A). The code also facilitates generation of a structure with specific atomic concentrations via the use of the optional input file `conc.in` (see `genrndstr -h` and table 2). For example, in a ternary system, if the composition of one of the atomic species is determined in the `conc.in` file, the remaining two atomic species composition are picked randomly. The repeated use of `genrndstr` in this case produces a binary section on the ternary system.

3.3. Constrained relaxation of a structure

In this step of the process, a special first-principles structural relaxation is performed. In this special relaxation, the atomic structure is constrained to remain in the vicinity of the initial atomic structure, i.e. in ζ_σ. A first-principles code is invoked automatically in this step, where the placeholder `xxxx` stands for the first-principles code (e.g. `vasp`). In the current version of the P^4 toolkit, the interface with `vasp` code [30, 31] is implemented. All necessary parameters for the first-principles code should be provided to the module inside a wrapper file called `xxxx.wrap` (see table 3). This file contains the settings needed for a standard electronic structure calculation and should be placed in the same directory as the augmented lattice and the unrelaxed structure input files (e.g. `lat.in` and `str.in`). Wrapper files needed for other calculations in the process, like the force-constant calculation of the relaxed structure and force calculation, are generated from the `vasp.wrap` file by running the following command.

```
vcrelax_vasp -mk
```

In the next step, the confined structural relaxation is performed by using the following command,

```
vcrelax_vasp -vc -vcop "options" -fc
```

where the `-vc` option conducts the confined relaxation process and the `-fc` option performs the force-constant calculation on the relaxed structure. The options for the `vcminimizer` command can be optionally passed to the `vcrelax_vasp` command by enclosing them in double quotation marks following the `-vcop` tag. The prefix needed for the *ab-initio* code to run on a remote machine or in parallel (e.g. `mpirun`) can be passed to this module as the following.

```
vcrelax_vasp [options] command_prefix
```

In the relaxation process, only atomic positions are relaxed and the cell shape and volume are remained fixed. Any cell shape or volume relaxation should be performed on the unstable crystal structure and the local distorted structure prior to the steps described in Section 3.3. If the first-principles parameters are set in a way to relax the cell shape or volume of the structure, the `vcminimizer` module generates the "`Change in supercell shape`" error. Moreover, the cell shape and volume of the unstable lattice and distorted crystal structure should be identical. The best practice is to first identify the local distorted structure by exploring the *ab inito* energy surface along a specific distortion path (for example, see Ref. [5, 7]). Subsequent to determining the local distorted structure, one should relax the cell shape and volume (and not the atomic positions) of the distorted structure and use that as the unit cell for `auglat` module, both for the unstable crystal structure and local distorted structure. If the unit cell for the unstable crystal structure and local distorted structure are not the same, the code will generate the ``The local distorted structure unit cell should be an integer multiple of high-symmetry lattice unit cell.'' error. Additionally, it is highly recommended that one uses the `genrndstr` module (following the `auglat` command) instead of generating the augmented lattice or the structure files manually. Otherwise, unexpected errors might be observed in `vcrelax_vasp` or `mcmc`, due to inconsistent input lattice and structure files. For example, one can encounter the "`The structure is not initially inside the Voronoi cell.`" error if the atomic positions in the structure file and augmented lattice files are not the same.

While all the steps in the confined relaxation process are performed automatically by this module, it is useful to describe these steps in more details. Initially, the first-principles code performs an ionic step calculation to get the energy and atomic forces acting on the unrelaxed structure. Subsequently, the `vcminimizer` command (see `vcminimizer -h`) is invoked to determine the next atomic positions according to gradient descent optimization method. The value of the step size is passed to the code via the `-vcop "options"`. The optimization process differs from a regular gradient descent algorithm where the ordinary steepest descent leads the atomic positions outside ζ_σ. As indicated in Fig. 3, in such a case three possibilities exist: (i) some atoms cross a plane boundary in the tridimensional space, (ii) some atoms cross an edge (i.e. intersection of two plane boundaries) of the Voronoi cell in which they are confined, or (iii) some atoms are trapped at a corner (i.e. intersection of three or more plane boundaries). These cases can occur simultaneously to different atoms in the structure. In the first case, the steepest descent direction is projected along the boundary plane, as illustrated in Fig.3(c). In the second case, the steepest descent direction is projected along

the two intersecting plane boundaries, which ensures the remaining of the atomic positions inside the Voronoi cell (see Fig.3(d)). In the third case, the simultaneous projection of the steepest descent direction along the intersecting planes results in trapping of the atoms at the corner. After the search direction is determined by the `vcminimizer` module, the first-principles code is performed consequently in order to obtain the energy and forces for the next atomic positions. This process is conducted iteratively until the desired accuracy (passed to the `vcrelax_xxx` by the `-etol` option) is reached. The relaxed structure is written to `str_relax.out` file and the energy and atomic forces are written to `energy_relax` and `force_final.out`, respectively. If the `-fc` is passed to `vcrelax_vasp` command, the force-constant is calculated for the relaxed structure using the finite difference method implemented in `vasp`. The numerical parameters for the force constant calculation is in the `vaspfc.wrap`, which is generated by the `vcrelax_vasp -mk` command. The first-principles code parameters can be modified in their corresponding wrap files. The matrix of second-order partial derivatives of energy (force-constant) for the relaxed structure is written to `hessian.out` by this module. Additionally, phonon eigenvalues and eigenvectors are written to the `eigenvalues.out` and `eigenvectors.out` files, respectively. All the information about the constrained relaxation process is written to `vcminimizer.log` file.

3.4. Constrained vibrational free energy of the relaxed structure

In this step, the code computes the free energy of the system constrained to ζ_σ, which is denoted by F^*_σ in Eq. 2. This module adiabatically switches from a "reference" system to the real system through some intermediate steps. To generate the intermediate states that linearly switches between the "reference" and real systems, the following command is conducted in the parent directory, where the input files are located (see `mcmc -h`).

```
mcmc -gip -ip=[integration points file name]
```

The `-gip` option generates a subdirectory for each integration point (i.e. intermediate state) defined in the file passed to the code by the `-ip` option. If the `-ip` option is not specified, the 5-point Gaussian quadrature in [0 1] domain is used by default to generate the intermediate states.

As indicated in Fig. 4, for each intermediate state, the potential energy surface is defined as a linear interpolation between the real state (quadratic energy surface around the relaxed atomic structure , $\boldsymbol{x}^r_\sigma$) and the "reference" state (chosen to be mechanically stable), using the quadrature abscissa as the interpolation parameter. The "reference" system is defined as a stiff harmonic potential basin with its minimum at the unrelaxed atomic position, $\boldsymbol{x}^u_\sigma$. By default, the curvature of the harmonic well is set to 20 eV/Å/Å, which can be changed by passing the `-c` option.

The constrained vibrational free energy difference between the real and "reference" systems is the integration of the ensemble-averaged potential energy difference between the real and the "reference" systems along the switching path. The canonical average of potential energy difference between the real and the "reference" systems is obtained by performing a **M**onte **C**arlo **M**arkov **c**hain (MCMC) sampling in each subdirectory by conducting the following command.

```
cd [subdirectory name]
mcmc -r [options]
```

The sampling is conducted until convergence (determined by the `-etol` option) is reached in the energy difference, and the `denergy` file is written to each subdirectory. Additionally, the value of the ratio of MCMC states that are inside ζ_σ to the total number of MCMC states is sampled by launching the `mcmc -r [options]` command in `ratio_ref` subdirectory. In this subdirectory, the non-constrained canonical sampling is performed using the "reference" state energy surface. The `mcmc` command can be performed in the parallel mode via using the `mpi` command as following:

```
[mpicommand] [options] mcmc [options]
```

The `mcmc` code provides guidelines to facilitate the convergence of the sampling. The `mcmc -test` command performs a test Markov chain sampling in order to determine the most efficient burn-in period and gap period parameters. One can perform the test prior to running the Markov chain sampling for a system and pass the estimated parameters to the `mcmc -r` command via the existing options. The burn-in period is the number of steps after which the Markov

chain reaches the target or stationary distribution. The gap-period (denoted by m) determines the number of steps that are excluded from the Markov chain averaging. The process of including every m^{th} step ensures that the Markov chain is uncorrelated. It is also possible to run several independent Markov chain sampling on a given system in order to assess the best parameters of the Markov chain via standard empirical diagnosis methods [32].

Finally, the constrained vibrational free energy associated with ζ_σ (see Eq.2) is obtained by running the following command in the parent directory.

```
mcmc -fvib
```

The final constrained vibrational free energy is written to the file `fvib` in the parent directory.

3.5. Cluster expansion of constrained vibrational free energy

The vibrational free energy for the unstable crystal structure is the canonical average over different configurations on the augmented lattice (see Eq. 1). Traditionally, the cluster expansion method defines the energetics of a system in multicomponent alloys by specifying the energy associated with any atomic arrangement on a given lattice. Here, the constrained vibrational free energy, F^*_σ, rather than the energy, is represented by a cluster expansion for any atomic arrangement on the augmented lattice.The unknown parameters of the cluster expansion (the ECIs) can then be determined by fitting them to the vibrational free energy of a relatively small number of configurations obtained through the aforementioned steps, using the P^4 toolkit. For a number of configuration structures, e.g. defined in `str.in`, and their corresponding vibrational free energy, `fvib`, the following command from the `ATAT` toolkit can be used to fit a cluster expansion.

```
clusterexpand fvib
```

The above command generates a file (`fvib.eci`) including ECIs associated with the clusters in the `clusters.out` file. Prior to this command, one has to generate the cluster file, `clusters.out`, via the `corrdump -clus -2=[`r_2`] ... -6=[`r_6`]` command in `ATAT` (for more details see `corrdump` command help in `ATAT` manual). Alternatively, one can use the `mmaps` command in `ATAT` to gradually construct an increasingly more accurate cluster expansion, which generates both the cluster file, `clusters.out`, and the fitted parameters, `eci.out`. Additionally, the `mmaps` command provides the `-crf` option for user-defined correlation function for the cluster expansion.

To obtain the canonical ensemble of the configurational vibrational free energy, the following command form `ATAT` toolkit performs a Monte Carlo sampling on the provided cluster expansion:

```
memc2
```

There are many options and input files that should be set to use the `memc2` code. One can refer to Ref. [33] for more details on these options. To prevent `memc2` code from generating configurations in which more than one atom occupy a "group" of sites, one can specify (rather than fitting) those ECIs that correspond to clusters formed by sites inside each "group". Additionally, one can define any arbitrary correlation function (see `corrdump -h` from `ATAT` for more details) to facilitates this goal. In section 4, more details are discussed on how to perform such a task. Moreover, one has to start the Monte Carlo sampling on the cluster expansion from a starting temperature with a known value for free energy (see Eq. 3 in Ref. [33]). Common choices are high temperature, where mean field approximation holds, or low temperature, where low temperature expansion can be used. The integration path for `memc2` should be chosen in a way that no phase transition is encountered along the path [33].

4. Guidelines for use in solid solutions

In this section, the input files and steps described in section 3 are illustrated for the Ni-Ti binary system in the B2 phase as a prototypical example for solid solutions. Table 1 represents the high-symmetry lattice and a nearby distorted structure files. The following command writes the augmented lattice to the `lat.in` file.

```
auglat -l=hs_lat.in -loc=str_loc.in -ol=lat.in
```

We generate an atomic structure with a 3×3×3 supercell of the unit cell defined in `hs_lat.in`, using the generated

hs_lat.in	str_loc.in
2.99 2.99 2.99 90 90 90	2.99 2.99 2.99 90 90 90
1.0 0.0 0.0	1.0 0.0 0.0
0.0 1.0 0.0	0.0 1.0 0.0
0.0 0.0 1.0	0.0 0.0 1.0
0 0 0 Vac,Ti,Ni	0.1 0.1 0.1 Ti
0.5 0.5 0.5 Vac,Ti,Ni	0.4 0.4 0.4 Ni

Table 1: Input files passed to the `auglat` command to generate the augmented lattice for a high-symmetry lattice and a nearby low-symmetry distorted structure. `hs_lat.in` file and `str_loc.in` represent the B2 lattice and a distortion along the trigonal distortion path of the B2 structure for NiTi, respectively.

augmented lattice in the `lat.in` file as an input to the `genrndstr` command. The input files for the following command are presented in table 2.

```
genrndstr -lhs=hs_lat.in -laug=lat.in -os=str.in -ss=3,3,3
```

We use the following command to relax the atomic position of the unrelaxed structure in `str.in`, having a wrap-

lat.in	conc.in
2.99 0 0	Ti=0.52
0 2.99 0	Ni=0.48
0 0 2.99	
1 0 0	
0 1 0	
0 0 1	
0.1 0.1 0.1 Vac,Ti,Ni	
0.4 0.4 0.4 Vac,Ti,Ni	
0.1 0.1 0.9 Vac,Ti,Ni	
0.4 0.4 0.6 Vac,Ti,Ni	
0.1 0.9 0.1 Vac,Ti,Ni	
0.4 0.6 0.4 Vac,Ti,Ni	
0.1 0.9 0.9 Vac,Ti,Ni	
0.4 0.6 0.6 Vac,Ti,Ni	
0.9 0.1 0.1 Vac,Ti,Ni	
0.6 0.4 0.4 Vac,Ti,Ni	
0.9 0.1 0.9 Vac,Ti,Ni	
0.6 0.4 0.6 Vac,Ti,Ni	
0.9 0.9 0.1 Vac,Ti,Ni	
0.6 0.6 0.4 Vac,Ti,Ni	
0.9 0.9 0.9 Vac,Ti,Ni	
0.6 0.6 0.6 Vac,Ti,Ni	
1 1 1 Vac,Ti,Ni	
0.5 0.5 0.5 Vac,Ti,Ni	

Table 2: Input files for the `genrndstr` command to generate a random atomic structure on the augmented lattice. `lat.in` file represent the augmented lattice generated by `auglat` and `conc.in` is an optional input file to determine the concentration of atomic species.

per file `vasp.wrap` with first-principles parameters (see table 3) and augmented lattice in `lat.in` as input files.

```
vcrelax_vasp -mk
vcrelax_vasp -vc -etol 0.01 -fc
```

The above command writes the relaxed atomic structure, its energy, force and force-constant to `str_relax.out`, `energy_relax`,

force_final.out and hessian.out, respectively. Additionally, the eigenvalues and eigenvectors of the dynamical matrix are written to eigenvalues.out and eigenvectors.out files.

vasp.wrap
[INCAR]
PREC = high
ISMEAR = 1
SIGMA = 0.1
NSW=40
IBRION = 2
ISIF = 3
KPPRA = 1000
USEPOT = PAWPBE
DOSTATIC

Table 3: An example of vasp.wrap file passed to the vcrelax_vasp command that determines the first-principles calculation parameters. All the tags are ordinary tags used in vasp code except for the KPPRA, USEPOT and DOSTATIC that are tags in the ezvasp module in ATAT.

To obtain the vibrational free energy associated with the structure str.in, first we generate the intermediate states for the adiabatic switching by running "mcmc -gip" and then we run the following command in each subdirectory.

```
mcmc -r -T=400
```

The above command can be performed in parallel using the mpirun or mpiexec. When all calculations are done in the subdirectories, the vibrational free energy is written to fvib file by running "mcmc -fvib" in the parent directory.

To fit a cluster expasion to any number of data point obtained via the above commands, we use the following command.

```
mmaps -crf="half" -pn=fvib
```

The -crf option defines the correlation function for each cluster (see corrdump -h in ATAT for details on default definition of cluster functions). When using an augmented lattice, a vacancy should be present as an atomic species in the lattice file to ensure the occupation of a "group" of sites by only one atom. Therefore, a binary system with mechanical instabilities is considered as a ternary system when using cluster expansion and Monte Carlo sampling of configurations. Similarly, a ternary system with phonon instabilities is considered as a quaternary in the P^4 context, etc. We used the ternary cluster functions defined in table 4, which associates the value zero to the occupation variable when a vacancy is present on the atomic site and a nonzero value in the presence of any other atomic species (see atat/src/corrskel.c++ for details on defining user-defined correlation functions). This definition enables a transparent way to assign large values (in this example 1000 eV) for ECIs of clusters formed inside "group" of atoms to prevent the occupation of each "group" by more that one atomic species. The Monte Carlo sampling of different configura-

occupation variable		0	1	2
cluster function	1 '0'	0	1/2	1
	1 '1'	0	1	1/2

Table 4: Definition of the ternary cluster functions, "half", passed to the mmaps command to generate the clusters and the effective cluster interactions (ECIs) files.

tions on the augmented lattice is performed using the following command from ATAT toolkit.

```
memc2 -keV -crf=half -is=gs_str.out -er=9 -phi0=-29.3211 -tp=0.001
```

The gs_str.out is the structure file with the smallest fvib value. The -phi0 value is the free energy at high enough temperature (in this example 10^6 K), where we can assume that lattice sites are randomly occupied by atomic species.

According to the definition of cluster functions in table 4, for 50% composition picked randomly, the correlations for point clusters and pair clusters between sites in distinct "groups" are 0.0833 and 0.0069, respectively. The correlation for pair clusters formed between sites inside one "group" is 0.0. This is due to the fact that each "group" is occupied with only one atom, which has a non-zero occupation value, and the rest of sites in the group are occupied with vacancies, for which the occupation variables are zero. The vibrational free energy at high temperature is obtained by having the ECIs and the random correlation values according to Eq. 3. The entropy for the random state is obtained according to $k_B \log(w)$, where w is the number of configurational states available to each atom (in this example, w=18). The temperature and chemical potential values should be set in the `control.in` file to maintain the sampling in the `memc2` in the desired temperature and composition range. The `eci.out` file should include the fitted ECIs from the `mmaps` command and the predefined ECIs assigned to clusters formed in a "group" of sites.

5. Example

In this section, we calculate the free energy for mechanically unstable B2 phase of NiTi using the P^4 toolkit. Additionally, we calculate the free energy of the low temperature mechanically stable B19' phase via standard harmonic lattice vibration method. We obtain the equilibrium transition temperature (where the free energies of B2 and B19' coincide) and compare it with experimental measurements of martensitic transformation between B2 and B19' phases. For the B2 phase, all the calculation steps are similar to what is explained in section 4 expect that the atomic species for the high-symmetry lattice sites and the resultant augmented lattice are different. In table 1, the atomic species allowed on the corner lattice site (located at 0.0 0.0 0.0) are Vac, Ni and those allowed on the center lattice site (located at 0.5 0.5 0.5) are Vac,Ti. The nearby distortion is determined by exploring the *ab-initio* energy surface along unstable phonon modes (see Ref. [7] for more details). For the first-principles calculation invoked by `vcrelax_vasp`, we use Vienna Ab-initio Simulation Package (VASP) [30, 31]. In this example, the ion-electron interaction is described by the projector augmented wave (PAW) method [34, 35], with energy cutoff of 269.6 eV and the generalized gradient approximation (GGA) [36] is used for exchange-correlation functional. The Brillouin zone integration is performed using a $4 \times 4 \times 4$ Monkhorst-Pack mesh for a $3 \times 3 \times 3$ supercell of B2 phase and an $8 \times 8 \times 8$ Monkhorst-Pack mesh for a $2 \times 2 \times 2$ supercell of B19' phase. This choice of parameters ensures that the energy values are converged with an accuracy of 1 meV/atom. The lattice constant used for the cubic B2 phase is $a = 2.99$Å and the lattice parameters used for the B19' phase are $a = 2.89$Å, $b = 4.63$Å, $c = 4.09$Å, $\alpha = 90°$, $\beta = 90°$ and $\gamma = 97.8°$.

Fig. 5 shows the Helmholtz free energy of the B2 phase of ordered NiTi at different temperatures, obtained by the P^4 toolkit. For the B2 phase, the free energy value at each temperature is obtained by fitting a cluster expansion with 51 pair clusters (excluding pair clusters formed in a "group" of sites) on 112 data points (where each data point includes an atomic structure `str.in` and its `fvib`). The vibrational free energy, `fvib`, for each configuration is obtained using the `mcmc -r` command only at one temperature, T_1 (here at T_1=600K). Constrained vibrational free energy at any other temperature T_2 is simply calculated by knowing `fvib` at T_1 and by using the well-known thermodynamic integration

$$\frac{F^*(T_2,\sigma)}{T_2} = \frac{F^*(T_1,\sigma)}{T_1} + \int_{T_1}^{T_2} \langle U(T) \rangle \, d(1/T),$$

where U is the internal energy and the ensemble average is taken over the domain ζ_σ (see Eq. 6 in Ref. [5]). The average internal energy of the system can be obtained by using the `-u` option in the `mcmc` command (see `mcmc -h` for details).

For the B19' phase, free energy is calculated using a harmonic approximation, as implemented in `fitfc` module in `ATAT`. The obtained free energy values for different temperatures are illustrated in Fig. 5. The free energy curves for the B2 and B19' phases coincides at $T = 258$K, as shown in Fig. 5. Other studies have reported experimental measurements of martensitic transformation in NiTi, which consist of four characteristic martensitic transformation temperatures; martensite start (M_s), martensite finish (M_f), austenite start (A_s) and austenite finish (A_f) temperatures [37, 38]. We compare our calculated equilibrium transition temperatures with the commonly-used value of $T_0 = (M_s + A_f)/2$, where A_f and M_s are experimentally measured. The transition temperature of 258 K is in good agreement with $T_0 = 310$K in Ref. [37] and $T_0 = 334$K of Ref. [38]

6. Conclusion

In this work, we presented a set of software tools which facilitates free energy calculation of solid phases with phonon instabilities that exist above certain temperatures due to dynamic stabilization. The advantage of the developed software tools is twofold. First, they provide a simple and robust method to extend the efforts towards including anharmonic vibrational effects in free energy to solid solution and alloys. Second, the generated free energy models can provide very good starting points for complex thermodynamic assessment for `CALPHAD` practitioners.

The presented software tools are among the first efforts to include anharmonic finite temperature effects into thermodynamic assessment via first principles calculations, while major efforts in the *ab initio* field are focused on absolute zero temperature calculation. Some aspects of the proposed scheme could be improved in the future. One major area of possible improvement is hessian calculation via approximate updating schemes, where the first-principles calculation are the most computationally intensive. The tools presented herein have been implemented in the Piecewise Polynomial Potential Partitioning (P^4) software, which interfaces with the Alloy Theoretic Automated Toolkit (ATAT).

7. Acknowledgments

This work is supported by the National Science Foundation under grant DMR-1835939 and by the Office of Naval Research under grant N00014-17-1-2202 and by Brown University through the use of the facilities of its Center for Computation and Visualization. This work used the Extreme Science and Engineering Discovery Environment (XSEDE), which is supported by National Science Foundation grant number ACI-1548562.

Appendix A. Structure and lattice file formats

Both the lattice and the structure files have a similar structure, which is indicated in table A.5. First, the coordinate system is specified, either as coordinate vector lengths a, b and c and the angles between them α, β and γ or as vectors in $\boldsymbol{x}$, $\boldsymbol{y}$ and $\boldsymbol{z}$ directions. In the former case the coordinate system parameters are written in the first line and in the latter case the coordinate vectors are written in the first three lines. In the next three lines the lattice vectors $\boldsymbol{u}$, $\boldsymbol{v}$ and $\boldsymbol{w}$ are listed, which are expressed in terms of the coordinate system. Atomic positions and types are given in the subsequent lines, which are also expressed in the same coordinate system as the lattice vectors. In the lattice file, the atom type is a comma-separated list of the atomic symbols that can occupy the corresponding lattice site. The atomic symbol 'Vac' or 'Va' is used to indicate a vacancy. In the structure file, the atom type is just a single atomic symbol which is among the atomic symbols given in the lattice file and vacancies do not need to be specified.

coordinate system	$[a]$ $[b]$ $[c]$ $[\alpha]$ $[\beta]$ $[\gamma]$	$[a_x]$ $[a_y]$ $[a_z]$ $[b_x]$ $[b_y]$ $[b_z]$ $[c_x]$ $[c_y]$ $[c_z]$
lattice vectors	$[u_x]$ $[u_y]$ $[u_z]$ $[v_x]$ $[v_y]$ $[v_z]$ $[w_x]$ $[w_y]$ $[w_z]$	
atom/site positions and types	[atom1a] [atom1b] [atom1c] [atom1type] [atom2a] [atom2b] [atom2c] [atom1type] etc.	

Table A.5: Structure and lattice file formats used in the P^4 software.

[1] A. van de Walle, G. Ceder, Automating first-principles phase diagram calculations, Journal of Phase Equilibria 23 (2002) 348.
[2] Y. Wang, Z.-K. Liu, L.-Q. Chen, Thermodynamic properties of Al, Ni, NiAl, and Ni3Al from first-principles calculations, Acta Materialia 52 (2004) 2665 – 2671.
[3] G. Ghosh, A. van de Walle, M. Asta, First-principles calculations of the structural and thermodynamic properties of bcc, fcc and hcp solid solutions in the Al–TM (TM=Ti, Zr and Hf) systems: A comparison of cluster expansion and supercell methods, Acta Materialia 56 (2008) 3202 – 3221.
[4] Z.-K. Liu, First-principles calculations and calphad modeling of thermodynamics, Journal of Phase Equilibria and Diffusion 30 (2009) 517.
[5] S. Kadkhodaei, Q.-J. Hong, A. van de Walle, Free energy calculation of mechanically unstable but dynamically stabilized bcc titanium, Phys. Rev. B 95 (2017) 064101.
[6] W. Petry, A. Heiming, J. Trampenau, M. Alba, C. Herzig, H. R. Schober, G. Vogl, Phonon dispersion of the bcc phase of group-IV metals. I. bcc titanium, Phys. Rev. B 43 (1991) 10933–10947.
[7] S. Kadkhodaei, A. van de Walle, First-principles calculations of thermal properties of the mechanically unstable phases of the PtTi and NiTi shape memory alloys, Acta Materialia 147 (2018) 296 – 303.

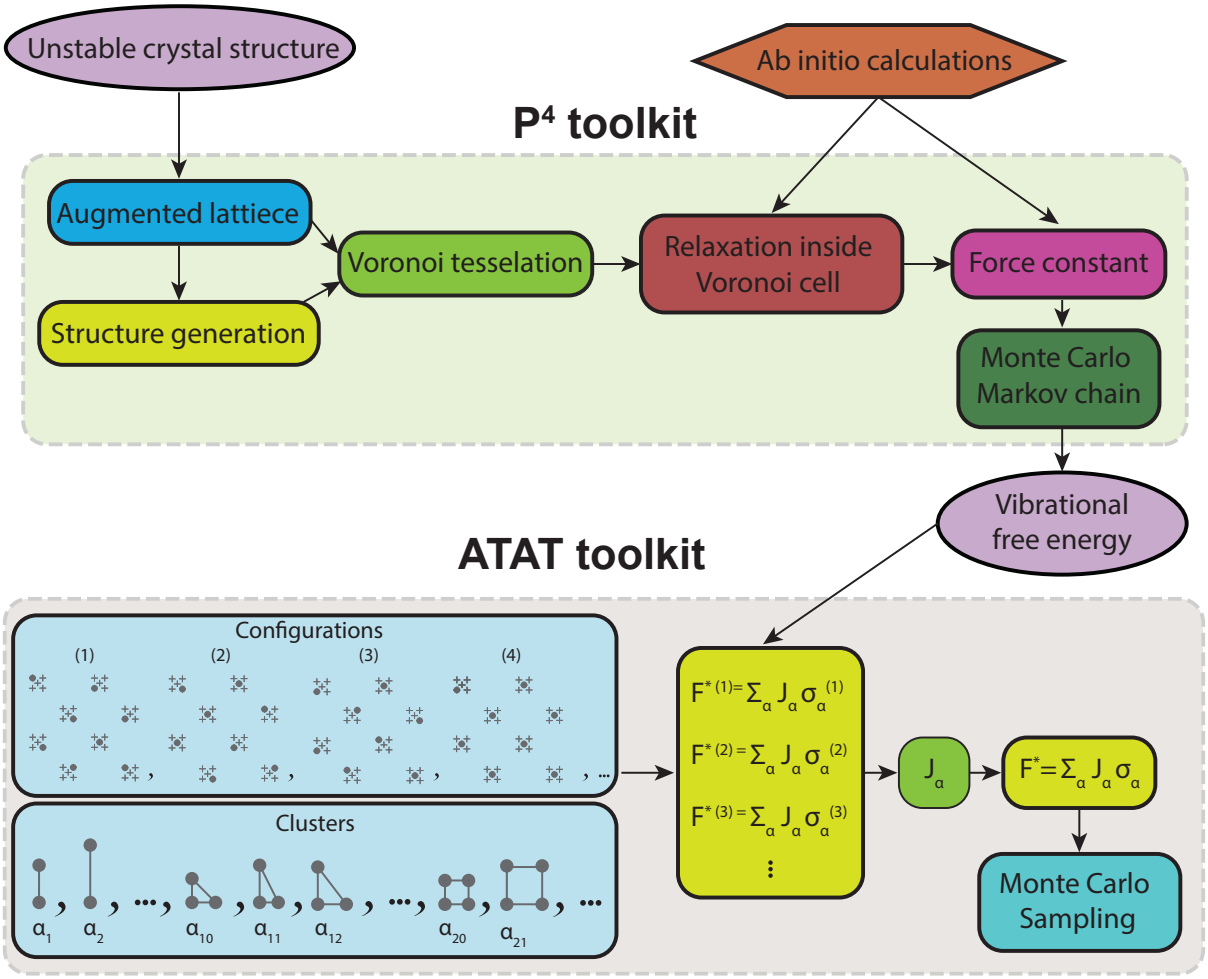

Figure 1: **Computational steps in the P^4 toolkit and the transfer of P^4 output to `ATAT` as input**. In the P^4 toolkit, the augmentation of the lattice is performed using the `auglat` module and the structure generation on the augmented lattice is performed using the `genrndstr` module. `vcrelax_xxxx` module perform first-principles calculations to obtain the relaxed structure confined in the Voronoi cell and force-constant of the relaxed structure. The Monte Carlo Markov chain sampling is performed by using the `mcmc` module. In the `ATAT` toolkit, a cluster expansion of the calculated vibrational free energies for a number of configurations can be obtained using the `mmaps` or `clusterexpand` module. The Monte Carlo sampling for the cluster expansion can be performed using the `memc2` module.

[8] J. B. Haskins, J. W. Lawson, Finite temperature properties of NiTi from first principles simulations: Structure, mechanics, and thermodynamics, Journal of Applied Physics 121 (2017) 205103.

[9] X. Huang, G. J. Ackland, K. M. Rabe, Crystal structures and shape-memory behaviour of NiTi, Nature Materials 2 (2003) 307–311.

[10] A. P. Mirgorodsky, M. B. Smirnov, P. E. Quintard, Lattice-dynamical study of the cubic-tetragonal-monoclinic transformations of zirconia, Phys. Rev. B 55 (1997) 19–22.

[11] Y. Zhang, X. Ke, P. R. C. Kent, J. Yang, C. Chen, Anomalous lattice dynamics near the ferroelectric instability in PbTe, Phys. Rev. Lett. 107 (2011) 175503.

[12] S. Kadkhodaei, Piecewise Polynomil Potential Partitioning (P4) toolkit, 2018. https://go.uic.edu/p4 and https://doi.org/10.26300/zs0n-2c84.

[13] A. van de Walle, G. Ceder, The effect of lattice vibrations on substitutional alloy thermodynamics, Rev. Mod. Phys. 74 (2002) 11–45.

[14] J. Sanchez, F. Ducastelle, D. Gratias, Generalized cluster description of multicomponent systems, Physica A: Statistical Mechanics and its Applications 128 (1984) 334 – 350.

[15] B. Grabowski, L. Ismer, T. Hickel, J. Neugebauer, *Ab initio* up to the melting point: Anharmonicity and vacancies in aluminum, Phys. Rev. B 79 (2009) 134106.

[16] A. I. Duff, T. Davey, D. Korbmacher, A. Glensk, B. Grabowski, J. Neugebauer, M. W. Finnis, Improved method of calculating *ab initio*

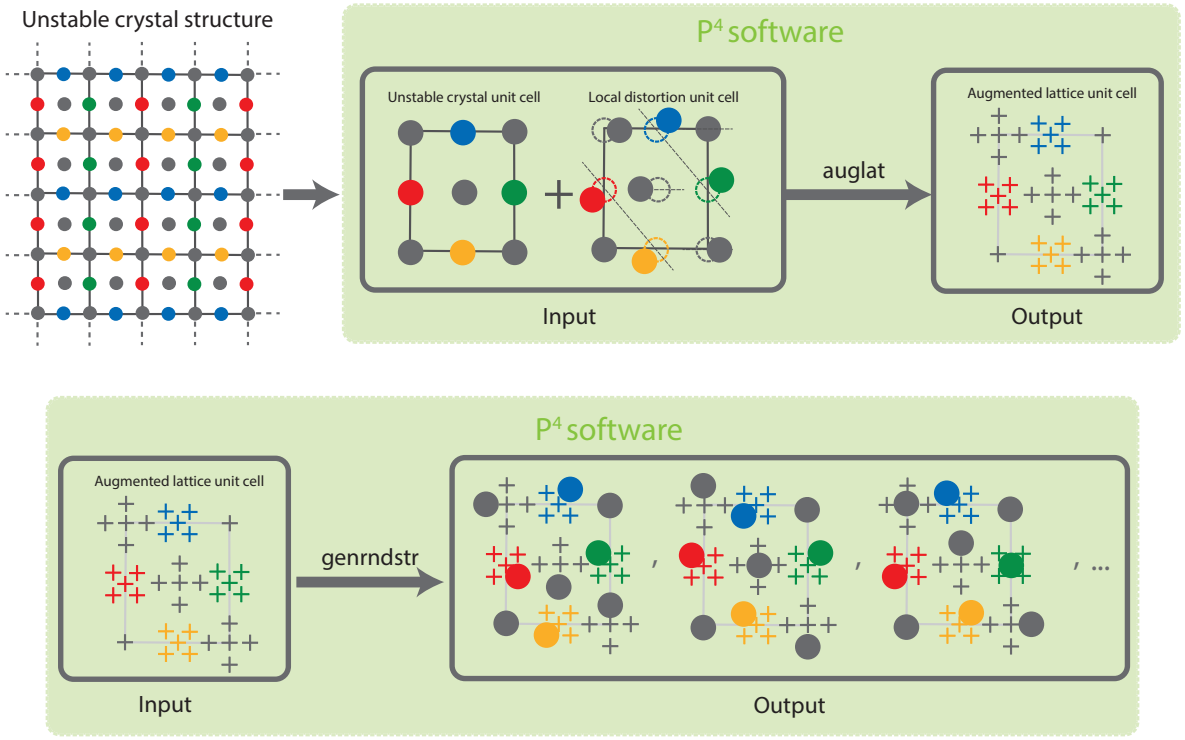

Figure 2: **Illustration of augmented lattice creation and structure generation on the resulting augmented lattice by the P^4 toolkit.** The `auglat` module in the P^4 package needs the unstable crystal structure and the structure of a local distortion in order to create the augmented lattice. Given one possible nearby distortion, the code will generate the augmented lattice by considering all distortions that are symmetrically equivalent to the given distortion. The `genrndstr` module in the P^4 package needs the augmented lattice file in order to randomly generate a possible arrangement of allowed atomic species on each "group" of augmented lattice.

high-temperature thermodynamic properties with application to ZrC, Phys. Rev. B 91 (2015) 214311.
[17] P. Souvatzis, O. Eriksson, M. I. Katsnelson, S. P. Rudin, Entropy driven stabilization of energetically unstable crystal structures explained from first principles theory, Phys. Rev. Lett. 100 (2008) 095901.
[18] P. Souvatzis, O. Eriksson, M. Katsnelson, S. Rudin, The self-consistent ab initio lattice dynamical method, Computational Materials Science 44 (2009) 888 – 894.
[19] I. Errea, M. Calandra, F. Mauri, Anharmonic free energies and phonon dispersions from the stochastic self-consistent harmonic approximation: Application to platinum and palladium hydrides, Phys. Rev. B 89 (2014) 064302.
[20] O. Hellman, I. A. Abrikosov, S. I. Simak, Lattice dynamics of anharmonic solids from first principles, Phys. Rev. B 84 (2011) 180301.
[21] O. Hellman, P. Steneteg, I. A. Abrikosov, S. I. Simak, Temperature dependent effective potential method for accurate free energy calculations of solids, Phys. Rev. B 87 (2013) 104111.
[22] O. Hellman, I. A. Abrikosov, Temperature-dependent effective third-order interatomic force constants from first principles, Phys. Rev. B 88 (2013) 144301.
[23] F. Zhou, W. Nielson, Y. Xia, V. Ozoliņš, Lattice anharmonicity and thermal conductivity from compressive sensing of first-principles calculations, Phys. Rev. Lett. 113 (2014) 185501.
[24] X. Ai, Y. Chen, C. A. Marianetti, Slave mode expansion for obtaining ab initio interatomic potentials, Phys. Rev. B 90 (2014) 014308.
[25] P. Souvatzis, Scaild, http://www.uquantchem.com/scaild.html, 2011.
[26] O. Hellman, N. Shulumba, http://ollehellman.github.io/page/index.html, 2011.
[27] N. Zarkevich, ThermoPhonon, https://lib.dr.iastate.edu/ameslab_software/2/, 2014.
[28] A. van de Walle, M. Asta, G. Ceder, The alloy theoretic automated toolkit: A user guide, Calphad 26 (2002) 539 – 553.
[29] A. van de Walle, Multicomponent multisublattice alloys, nonconfigurational entropy and other additions to the alloy theoretic automated toolkit, Calphad 33 (2009) 266 – 278. Tools for Computational Thermodynamics.
[30] G. Kresse, J. Furthmüller, Efficient iterative schemes for ab initio total-energy calculations using a plane-wave basis set, Phys. Rev. B 54 (1996) 11169–11186.

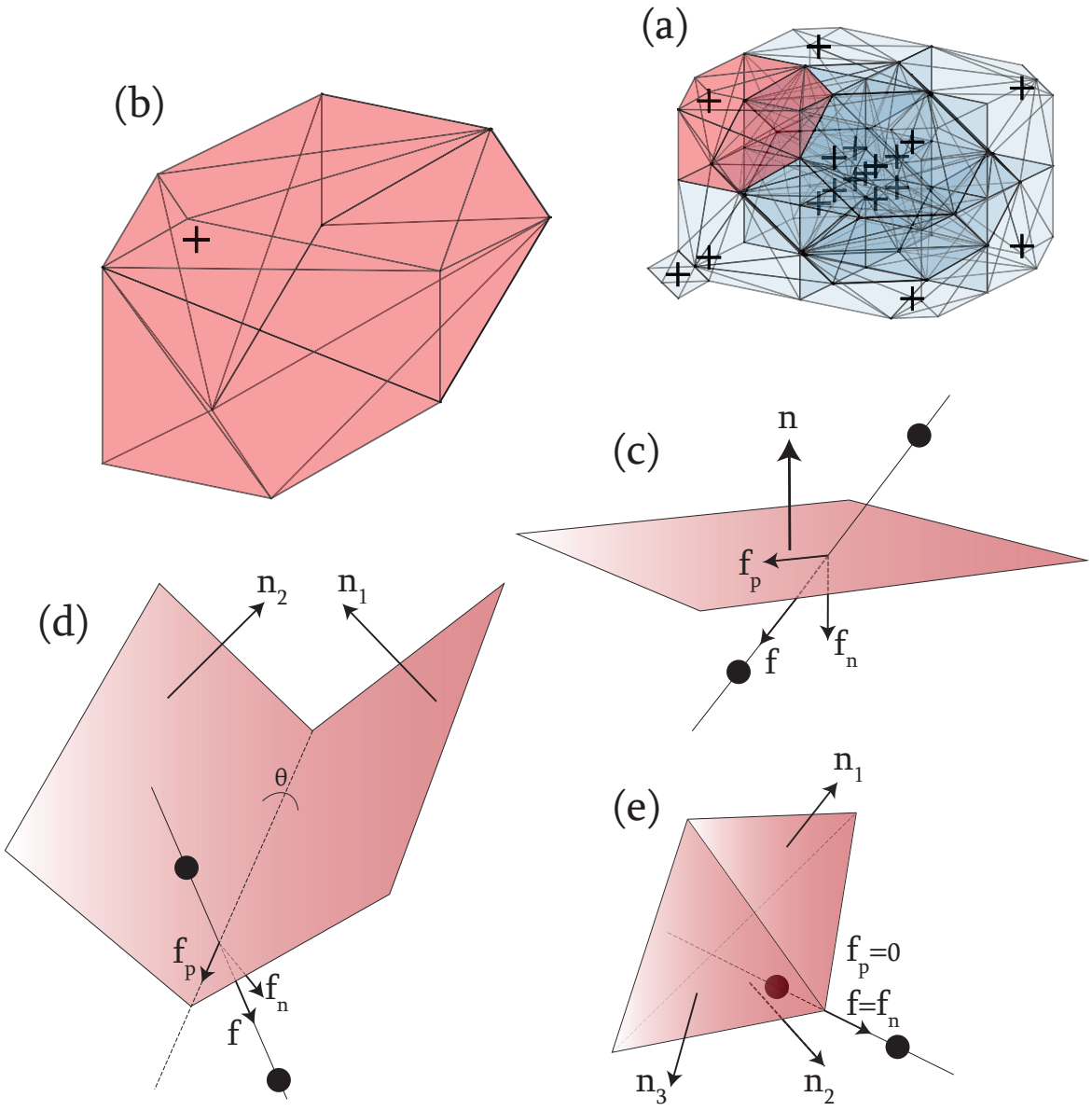

Figure 3: **Search direction determination for the relaxation process inside the Voronoi cell, implemented in the `vcrelax_xxxx` module.** (a) The augmented lattice sites and the Voronoi tessellation of the tridimensional space. (b) The Voronoi cell for a site in the augmented lattice. (c) Projection of the steepest descent search direction on a boundary plane of the Voronoi cell. (d) General non-orthogonal projection of the steepest descent search direction on an edge of the Voronoi cell. (e) General non-orthogonal projection of the steepest descent search direction on a corner of the Voronoi cell.

[31] G. Kresse, J. Furthmüller, Efficiency of ab-initio total energy calculations for metals and semiconductors using a plane-wave basis set, Computational Materials Science 6 (1996) 15 – 50.

[32] M. K. Cowles, B. P. Carlin, Markov chain monte carlo convergence diagnostics: A comparative review, Journal of the American Statistical Association 91 (1996) 883–904.

[33] A. van de Walle, M. Asta, Self-driven lattice-model monte carlo simulations of alloy thermodynamic properties and phase diagrams, Modelling and Simulation in Materials Science and Engineering 10 (2002) 521.

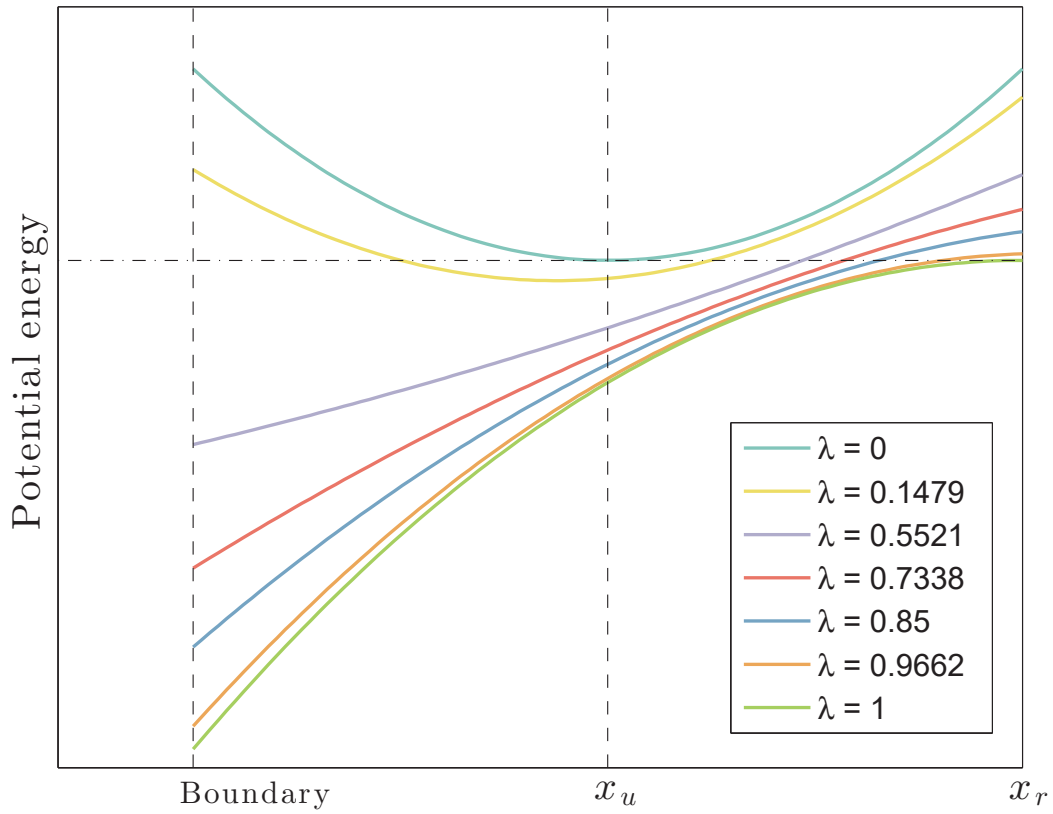

Figure 4: Linear interpolation of the potential energy surface between the "reference" potential ($\lambda = 0$) and the real potential ($\lambda = 1$) by interpolation parameter λ. In this illustrative example, λ values are obtained from the 5-point Gaussian quadrature abscissae. x_r is the relaxed atomic position confined in the Voronoi cell and x_u represents the unrelaxed atomic structure.

[34] P. E. Blöchl, Projector augmented-wave method, Phys. Rev. B 50 (1994) 17953–17979.
[35] G. Kresse, D. Joubert, From ultrasoft pseudopotentials to the projector augmented-wave method, Phys. Rev. B 59 (1999) 1758–1775.
[36] J. P. Perdew, Generalized gradient approximation for the fermion kinetic energy as a functional of the density, Physics Letters A 165 (1992) 79 – 82.
[37] K. Otsuka, X. Ren, Physical metallurgy of ti–ni-based shape memory alloys, Progress in Materials Science 50 (2005) 511 – 678.
[38] J. Khalil-Allafi, B. Amin-Ahmadi, The effect of chemical composition on enthalpy and entropy changes of martensitic transformations in binary niti shape memory alloys, Journal of Alloys and Compounds 487 (2009) 363 – 366.

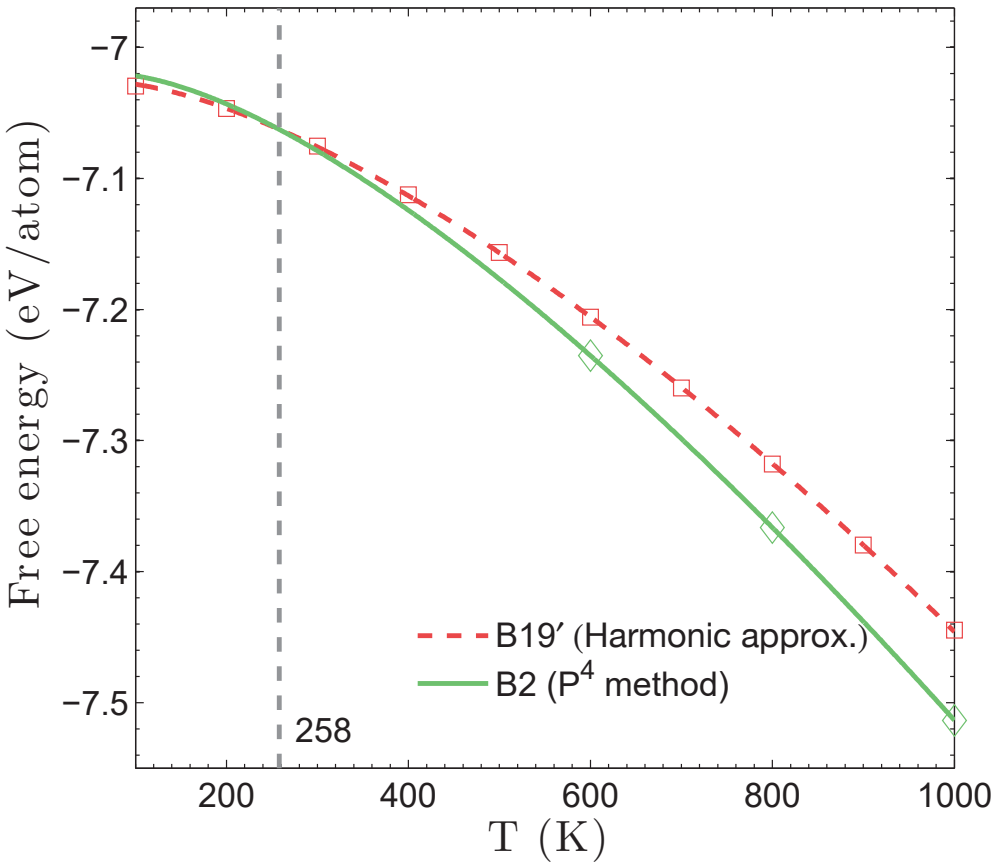

Figure 5: Helmholtz free energy for the B2 and B19' phases of NiTi. The free energy values for the B2 phase are calculated using the P^4 software toolkit and are depicted by green diamonds in the plot. The free energy values for B19' phase are calculated using the harmonic approximation implemented in the `fitfc` module in `ATAT` and are depicted by red squares. The free energy curves are least square fits to the free energy values in the form $c_1 + c_2T + c_3T^2 + c_4T \log T$, where T is temperature and c_1 to c_4 are the fit coefficients.